

Subnanosecond lifetime measurements in Y and Sr nuclei and the saturation of deformation near $A = 100$

H. Mach,^{(a),(b),*} F. K. Wohn,^(c) M. Moszyński,^{(a),(b)} R. L. Gill,^(a) and R. F. Casten^(a)

^(a)Brookhaven National Laboratory, Upton, New York 11973

^(b)Institute for Nuclear Studies, PL 05-400, Swierk-Otwock, Poland

^(c)Ames Laboratory, Iowa State University, Ames, Iowa 50011

(Received 24 July 1989)

Half-lives of 47(6) ps in ^{99}Y and 72(7) ps in ^{100}Y , measured by β - γ - γ coincidences, and intraband $M1/E2$ ratios give $M1$ strengths and g factors of the bands $\pi_{\frac{3}{2}}[422]$ in ^{99}Y , $\nu_{\frac{3}{2}}[411]$ in ^{99}Sr , and $\pi_{\frac{3}{2}}[422]\nu_{\frac{3}{2}}[411]$ in ^{100}Y . The results are in remarkable agreement with the simple picture of these nuclei as a deformed ^{98}Sr core plus one or two valence nucleons, thus indicating that the deformation saturates for $A \approx 100$ Sr and Y nuclei. This "early" saturation can be explained in terms of valence Nilsson orbitals.

Transitional and deformed nuclei in the neutron-rich region near ^{100}Zr are characterized by remarkable features, such as an extremely abrupt transition from spherical to highly deformed shapes. (Detailed discussions of the region are given in Ref. 1.) The abruptness of the shape transition has been attributed to subshell effects (for $Z=38,40$ and $N=56,58$) and the occupation by valence nucleons of orbitals for which a residual proton-neutron interaction is particularly effective in promoting a deformed nuclear shape. To probe this in detail, the properties of both the collective deformation and the states occupied by the valence nucleons need to be established.

Absolute transition rates provide essential information on the valence nucleon states in deformed $A \approx 100$ nuclei. For rotational bands in deformed even-even nuclei, the strongly enhanced $B(E2)$ values directly provide a measure of the collectivity of the core. In contrast, for rotational bands in deformed odd- A nuclei, it is the $B(M1)$ values that provide information on the single-particle state of the valence nucleon, and similarly for the states of each odd nucleon in deformed odd-odd nuclei.

The recent development of a method²⁻⁴ for fast-timing measurements using β - γ - γ coincidences makes it possible, for the first time, to systematically measure half-lives below 100 ps. The ^{99}Y and ^{100}Y half-lives presented here are the first such "short" half-lives to be reported for $A \approx 100$ nuclei. The main purpose of this article is to demonstrate the validity of a very simple picture for the structure of these nuclei, namely that the deformation of the even-even core (^{98}Sr) is constant, unaffected by the presence of one or two valence nucleons. In particular, we show that the intrinsic g factor g_K and quadrupole moment Q_0 for ^{99}Y , ^{99}Sr , and ^{100}Y deduced from their

half-lives and $M1/E2$ ratios are the values expected if all three nuclei have the same Q_0 and deformation as ^{98}Sr . This feature is an extension to odd- A and odd-odd nuclei of the idea of saturation of deformation recently deduced⁵ for even-even ^{98}Sr and ^{100}Sr . A second purpose is to show that g factors calculated with the Nilsson model for the indicated constant deformation are in excellent agreement with the g factors deduced from experiment.

The half-lives reported here for $^{99,100}\text{Y}$ were measured at the fission-product mass-separator TRISTAN at Brookhaven National Laboratory using the recently developed β - γ - γ fast-timing method. The method, which is discussed in detail in the technical publications,²⁻⁴ has already been used for lifetime measurements in the subnanosecond⁵ and low-picosecond⁶ ranges. Briefly, timing information is obtained from β - γ coincidences between a thin NE111A plastic and a small BaF_2 scintillator. An additional γ coincidence from a Ge detector is used to select the decay branch of interest. The electronics were optimized for E_γ (γ energy in BaF_2) of ~ 100 keV with timing resolutions (FWHM) of 290 ps at $E_\gamma = 65$ keV and 210 ps at $E_\gamma = 125$ keV. The half-lives were obtained by both a centroid-shift method and a deconvolution method.

In the centroid-shift method for direct β feeding of a level of interest, the meanlife ($T_{1/2}/\ln 2$) is given simply by the shift (or difference) between the centroid of the delayed time spectrum and the prompt centroid of the same E_γ . For indirect feeding (where the level of interest is fed by a γ ray from a higher level) the meanlife of interest is the difference between the centroid shift of the spectrum gated by the deexciting γ ray and the centroid shift of the spectrum gated by the feeding γ ray. Care must be taken

in calibrating the shifts, however, as even the centroids of prompt transitions are known to vary with E_γ ; this variation is called the prompt curve. Using a set of calibration lines, the shape of the prompt curve was obtained in the range $55 < E_\gamma < 809$ keV. This is a relative calibration. To get an absolute calibration, it is then necessary to determine the absolute position of the curve separately for each experiment ($A=99$ and 100). This was obtained by renormalizing the relative prompt curve (i.e., shifting it by a constant to make it overlap) with centroids selected from Compton spectra of high-energy ($E_\gamma > 1.0$ MeV) γ rays (in $A=99$ or $A=100$ data) assumed to be prompt.²⁻⁴

A $T_{1/2}$ of 72(8) ps for the 76-keV level in ^{100}Y was obtained from the centroid shift of the 898-65 (898-keV gate in Ge and 65-keV gate in BaF_2) spectrum, after subtracting the centroid shift of the 65-898 spectrum. The subtraction corrected for the small time delay ($T_{1/2} < 2$ ps) due to the 898 γ ray (and γ rays cascading into the 898 level) feeding the 76-keV level. Similarly, a $T_{1/2}$ of 46(6) ps for the 125-keV level in ^{99}Y was found using the 158-125 and 125-158 spectra and, independently, the 531-125 and 125-531 spectra. The corrections for the indirect feeding were 21(5) ps and 17(6) ps for the latter two sets, respectively. The deconvolution fits were done with a prompt response approximated by a Gaussian.² The uncertainties due to the assumption of such a simple functional form are included in the final errors. The results of such simple deconvolution analyses of the 531-125 and 898-65 spectra gave $T_{1/2}$ values of 71(9) ps and 51(13) ps, respectively, as shown in Fig. 1. These values are in good agreement with the centroid-shift results. As final numbers we adopt weighted average $T_{1/2}$ values of 72(7) ps and 47(6).

The half-lives presented here for $^{99,100}\text{Y}$, together with those recently reported for ^{98}Sr (Ref. 5) and ^{99}Sr (Ref. 7), provide enough information to determine $M1$ strengths of the lowest Nilsson orbitals ($\pi_{5/2}^-[422]$ for protons and $\nu_{3/2}^-[411]$ for neutrons). From the $M1/E2$ ratios in the associated bands in ^{99}Y and ^{99}Sr , the $E2$ components (thus the values of Q_0) can be deduced. Previous studies⁷⁻¹¹ of these nuclei revealed nearly rigid rotational bands. (The best example is the $5/2_-^-[422]$ band in ^{99}Y , for which eight levels of the band have been observed.⁹) The three bands of interest here appear to be excellent examples of strongly coupled axial rotors,⁷⁻¹² which justifies the use of the following strong-coupling equations in our determination of the $M1$ and $E2$ properties of these three bands.

The $B(E2)$ value of an intraband $I \rightarrow I-1$ transition in a rotational band is

$$B(E2) = \left[\frac{5}{16\pi} \right] e^2 Q_0^2 [3K^2(I-K)(I+K)] / [(I-1)I(I+1)(2I+1)]. \quad (1)$$

K is the projection of the angular momentum on the symmetry axis. The $B(M1)$ value for the same $I \rightarrow I-1$ cascade transition is, for a band with $K \neq \frac{1}{2}$,

$$B(M1) = \left[\frac{3}{4\pi} \right] \mu_n^2 (g_K - g_R)^2 K^2 (I-K)(I+K) / [I(2I+1)]. \quad (2)$$

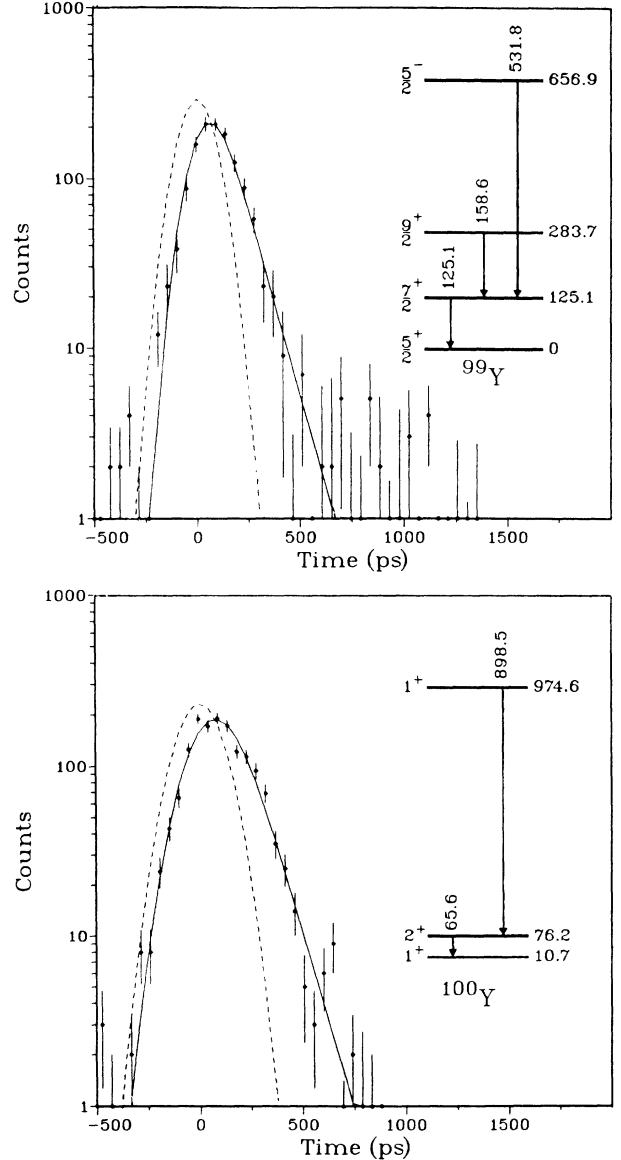


FIG. 1. *Top*: Delayed time spectrum for $7/2_+^+$ level of the $\pi_{5/2}^-[422]$ band in ^{99}Y obtained with a 125-keV BaF_2 gate and the sum of Ge gates at 158 and 531 keV. The χ^2 -fit curve is for $T_{1/2} = 51 \pm 13$ ps. The dashed curve is a Gaussian prompt distribution with $\text{FWHM} = 210$ ps for $E_\gamma = 125$ keV. *Bottom*: Delayed time spectrum for 2_+^+ level of the $\pi_{5/2}^-[422]\nu_{3/2}^-[411]$ band in ^{100}Y obtained with a 65-keV BaF_2 gate and a 898-keV Ge gate. The χ^2 -fit curve is for $T_{1/2} = 71 \pm 9$ ps. The dashed curve is a Gaussian prompt distribution with $\text{FWHM} = 290$ ps for $E_\gamma = 65$ keV.

μ_n is the nuclear magneton, g_K is the particle g factor, and g_R is the collective g factor. The γ -ray partial half-lives $T_{1/2}^{\gamma}(M1)$ and $T_{1/2}^{\gamma}(E2)$ are

$$T_{1/2}^{\gamma}(M1) = (3.94 \times 10^{-2} \text{ ps}) [\mu_n^2 / B(M1)] E_{\gamma}^{-3}, \quad (3a)$$

$$T_{1/2}^{\gamma}(E2) = (5.65 \times 10^{-2} \text{ ps}) [e^2 b^2 / B(E2)] E_{\gamma}^{-5} = T_{1/2}^{\gamma}(M1) / \delta^2. \quad (3b)$$

Note that $|\delta|$ (the magnitude of the $E2/M1$ mixing ratio) can be determined by the intensity ratio for cascade I_{γ} and crossover $I_{\gamma'}$ γ rays, since

$$I_{\gamma} / I_{\gamma'} = 2K^2(2I-1) / [(I+1)(I-1+K)(I-1-K)] (E_{\gamma} / E_{\gamma'})^5 (1 + \delta^{-2}). \quad (4)$$

With the cascade γ ray energy E_{γ} in MeV, the band parameter $(g_K - g_R) / Q_0$ is

$$(g_K - g_R) / Q_0 = 0.934 E_{\gamma} \delta^{-1} [(I-1)(I+1)]^{-1/2}. \quad (5)$$

Each level with $I \geq K+2$ in a band can yield a value of $|(g_K - g_R) / Q_0|$, which can thus be accurately determined. In terms of δ^2 , the total half-life $T_{1/2}$ is

$$T_{1/2} = T_{1/2}^{\gamma}(M1) / \{1 + \alpha_T(M1) + \delta^2 [1 + \alpha_T(E2)]\}. \quad (6)$$

The $\alpha_T(\sigma L)$ are total internal conversion coefficients for multipolarity σL .

For all three of the nuclei discussed here, the $E2$ component of the $K+1 \rightarrow K$ transition is very weak ($\sim 1\%$) compared to the $M1$ component. This gives large uncertainties in the deduced Q_0 values. (Indeed, for ^{100}Y the $K+2 \rightarrow K$ $E2$ γ ray was too weak to be observed,¹¹ thus a value of Q_0 cannot be deduced from the ^{100}Y data.) The present data thus give new information primarily on the $M1$ properties of the three bands. In the following, values of $g_K - g_R$ are deduced in two ways: One uses all of the data, both $T_{1/2}$ and $E2/M1$ ratios, and the other assumes a constant Q_0 and uses only the $T_{1/2}$ results. The latter is equivalent to assuming that the deformation β_2 does not change upon adding a proton, or a neutron, or both to the even-even core nucleus ^{98}Sr . The Q_0 used is that of the ^{98}Sr deformed band, recently found⁵ to be $Q_0 = 3.78(6)$ b, indicating a quadrupole deformation β_2 of 0.38(1) for axial symmetry.⁵ The four nuclei, $^{98,99}\text{Sr}$ and $^{99,100}\text{Y}$, are assumed to have the same β_2 and Q_0 .

Table I gives the values of the relevant $M1$ and $E2$ quantities that can be extracted from the $T_{1/2}$ and

$M1/E2$ data. [For the $|(g_K - g_R) / Q_0|$ value in ^{99}Sr , the intensity ratio from the $\frac{9}{2}^+$ band member was not used because γ rays with the same 125-keV energy as the $\frac{9}{2}^+ \rightarrow \frac{7}{2}^+$ transition occur in the decays of both ^{99}Rb and ^{99}Sr .] The presentation of the data and deduced quantities in Table I is arranged to facilitate later comparisons between quantities deduced without (third and fourth columns) and with (fifth and sixth columns) the assumption of a constant Q_0 . [For ^{100}Y , the values of $B(M1)$ and $|g_K - g_R|$ in the third and fourth columns were actually deduced by ignoring the $E2$ component, since the $E2$ component of the 65-keV transition is too weak ($< 0.4\%$ of the total) to significantly affect the deduced $M1$ properties.] The three $|(g_K - g_R) / Q_0|$ values in the sixth column can be regarded as predictions of the constant Q_0 assumption. They can be compared with the experimental $|(g_K - g_R) / Q_0|$ values given in the seventh column. The latter provide two independent tests of this assumption. Finally, the two Q_0 values in the eighth column, although they have much larger uncertainties, agree closely with the core value of 3.78(6) b.

Table II presents experimental, predicted, and calculated values of g_K . The values of g_R in the second column were obtained in accordance with analyses of the deformed rare earths. Thus g_R is given by Z/A for odd- Z ^{99}Y and $0.5Z/A$ for odd- N ^{99}Sr . A value of $0.75Z/A$ was assumed for odd-odd ^{100}Y . The g_K sign choices are given by the Nilsson orbitals and the fact that $g_{s\pi}$ (proton spin g factor) is positive and g_{sv} is negative. [For very large deformations, $g_{\pi} = (\Lambda_{\pi} + g_{s\pi} \Sigma_{\pi}) / |\Omega_{\pi}|$ and $g_{\nu} = (g_{sv} \Sigma_{\nu}) / |\Omega_{\nu}|$, where $|\Omega| = \Lambda + \Sigma$.] For an odd-odd nucleus, g_{π} and g_{ν} add according to $Kg_K = \Omega_{\pi} g_{\pi} + \Omega_{\nu} g_{\nu}$,

TABLE I. Experimental results for $M1$ and $E2$ quantities.

	$T_{1/2}$ (ps) ^a	$B(M1)$ (μ_n^2) ^b	$ g_K - g_R ^b$	$ g_K - g_R ^c$	$ (g_K - g_R) / Q_0 $ (b^{-1}) ^c	$ (g_K - g_R) / Q_0 $ (b^{-1}) ^d	Q_0 (b) ^e
^{99}Y	47(6)	0.38(5)	1.09(7)	1.11(7)	0.294(19)	0.281(21)	3.9(4)
^{99}Sr	580(90)	0.069(11)	0.69(5)	0.69(5)	0.183(20)	0.182(20)	3.8(5)
^{100}Y	72(7)	1.21(12)	4.11(20)	4.11(20)	1.09(5)		

^aPresent study for 125.1-keV $\frac{7}{2}^+$ level of ^{99}Y and 76.2-keV 2^+ level of ^{100}Y ; Ref. 7 for 90.8-keV $\frac{5}{2}^+$ level of ^{99}Sr .

^bDeduced from the $T_{1/2}$ values and the mixing ratios from refs. 8–10.

^cDeduced from the $T_{1/2}$ values and the assumption of a fixed Q_0 of 3.78(6) b; see text for further explanation.

^dDeduced from $M1/E2$ branching ratios; for ^{99}Y , average of 0.27(3) (Ref. 8) and 0.291(30) (Ref. 9) for $\frac{5}{2}[422]$ band; for ^{99}Sr , value obtained from $\frac{11}{2}^+$ member of $\nu_3^{\frac{3}{2}}[411]$ band (Ref. 10).

^eObtained from $|(g_K - g_R) / Q_0|$ of the seventh column and $|g_K - g_R|$ of the fourth column.

TABLE II. Summary of deduced intrinsic g factors g_K .

	g_R	$(g_K - g_R)^a$	g_K Expt. ^b	g_K Pred. ^c	g_K Calc. ^d
⁹⁹ Y	0.39	1.09(7)	1.48(7)		1.41
⁹⁹ Sr	0.19	-0.69(5)	-0.50(5)		-0.53
¹⁰⁰ Y	0.29	4.11(20)	4.40(20)	4.45(19)	4.32

^aFrom the fourth column of Table I; g_K sign given by Nilsson orbitals: $\pi_{\frac{5}{2}}[422]$ (⁹⁹Y), $\nu_{\frac{3}{2}}[411]$ (⁹⁹Sr), and $\pi_{\frac{5}{2}}[422]\nu_{\frac{3}{2}}[411]$ coupled to $K=1$ (¹⁰⁰Y).

^bDeduced from the data by adding g_R of the second column to $(g_K - g_R)$ of the third column.

^cPredicted g_K for ¹⁰⁰Y, given by $\Omega_{\pi}g_{\pi} + \Omega_{\nu}g_{\nu} = (\frac{5}{2})(1.48) + (-\frac{3}{2})(-0.50)$.

^d g_K calculated using Nilsson model; see text for Nilsson parameters.

where $K = \Omega_{\pi} + \Omega_{\nu}$. For the ¹⁰⁰Y $K=1$ case, $\Omega_{\pi} = +\frac{5}{2}$ and $\Omega_{\nu} = -\frac{3}{2}$. The three values of g_K in the fourth column are thus simple functions of the two parameters g_{π} (g_K for $\pi_{\frac{5}{2}}[422]$) and g_{ν} (g_K for $\nu_{\frac{3}{2}}[411]$). Thus the g_K values in the fourth column provide a simple test of the assumption that all three nuclei have the same β_2 , as this implies that there are only two independent g_K values: g_{π} and g_{ν} . (The g_K for a Nilsson orbital varies with deformation, as is shown quantitatively below.) The fifth column shows the value of g_K for ¹⁰⁰Y predicted using the ⁹⁹Y and ⁹⁹Sr g_K values of the fourth column. The predicted and experimental g_K values for ¹⁰⁰Y agree remarkably well, which strongly supports our constant deformation hypothesis.

Calculated values of g_K are given in the sixth column of Table II, obtained from g_{π} and g_{ν} values calculated at constant deformation using the Nilsson model. The core Q_0 of 3.78 b corresponds to a Nilsson deformation ϵ_2 of 0.33. (Ref. 15 gives relationships between Q_0 and the various types of deformation.) For ^{99,101}Y, many bands were observed and detailed particle-rotor calculations were made.^{8,12} The Nilsson parameters κ and μ were taken to be $\kappa=0.068$ and $\mu=0.51$, where μ is an average of 0.53 (⁹⁹Y) and 0.49 (¹⁰¹Y).^{8,12} [Nearly identical κ and μ values were recently shown to work well for both higher and lower Z (¹¹¹Ag in Ref. 13 and for $25 \leq Z \leq 31$ in Ref. 14).] A spin g factor $g_{s\pi} = g'g_{s\pi}^{\text{free}}$ ($g_{s\pi}^{\text{free}} = +5.586$) was used to calculate g_K . For deformed rare earths, g' ranges from 0.6 to 0.7, thus we assume a "best" g' of 0.65. To examine how g_K depends on ϵ_2 and μ , g_K was calculated for many choices of ϵ_2 and μ . For small ($\leq 10\%$) variations in the parameters, g_K is approximately given by

$$g_K = +1.41 + 0.88(g' - 0.65) \\ + 0.25(\epsilon_2 - 0.33) - 0.02(\mu - 0.51)$$

for $\pi_{\frac{5}{2}}[422]$. Note that g_K is very insensitive to μ , thus providing no information on μ . Note also that the experimental g_K of 1.48 would be given by the calculation for an acceptable g' value of 0.73.

For the $A \approx 100$ odd-neutron nuclei, there is more uncertainty in deducing a "best" set of Nilsson parameters since fewer bands have been clearly identified. However, the parameters $\kappa=0.66$ and $\mu=0.35$, deduced by interpolation,¹⁶ provide a reasonable choice for a "best" set. The

neutron spin g factor is $g_{s\nu} = g'g_{s\nu}^{\text{free}}$, and $g_{s\nu}^{\text{free}} = -3.826$. Nilsson calculations for parameters near this set were used to approximately express g_K via a linear expansion, getting

$$g_K = -0.53 - 0.81(g' - 0.65) \\ - 1.44(\epsilon_2 - 0.33) - 1.14(\mu - 0.35)$$

for $\nu_{\frac{3}{2}}[411]$. For this orbital, the value of g_K is quite sensitive to μ and ϵ_2 as well as g' . There is again excellent agreement between the calculated g_K of -0.53 and the experimental g_K of -0.50(5). Note that the g_K expansion makes it clear that using a g_K of -0.50 to determine a "best" value of μ would give a μ value that would depend strongly upon the values used for g' and ϵ_2 . In addition, the g_K value of -0.50 is more sensitive to the value assumed for g_R for $\nu_{\frac{3}{2}}[411]$ than for $\pi_{\frac{5}{2}}[422]$ (for which g_K was much larger). Therefore, rather than deducing a neutron value of μ in this way, we are content merely to show that our results are consistent with the μ of Ref. 16.

The ¹⁰⁰Y experimental g_K value confirms the opposite signs of g_{π} and g_{ν} . The sign is important, as the deduced negative sign for g_{ν} clearly excludes $\nu_{\frac{3}{2}}[422]$ which has a positive g_K . Based on a low $\log ft$ value in the decay of ¹⁰⁰Sr, the 10.7-keV 1^+ level in ¹⁰⁰Y was proposed¹¹ as the bandhead of a highly deformed band that should be mainly the $\pi_{\frac{5}{2}}[422]\nu_{\frac{3}{2}}[411]$ configuration (with higher 1^+ level being mainly $\pi_{\frac{5}{2}}[422]\nu_{\frac{3}{2}}[422]$). The present results prove that the 76.2-keV 2^+ level has all the properties consistent with being the 2^+ member of the $\pi_{\frac{5}{2}}[422]\nu_{\frac{3}{2}}[411]$ band.

There are four conclusions to be drawn from the tables: (1) the values of $|(g_K - g_R)/Q_0|$ predicted with a Q_0 of 3.78 b are in excellent agreement with the experimental values for ⁹⁹Y and ⁹⁹Sr, (2) the experimental Q_0 values for ⁹⁹Y and ⁹⁹Sr agree well with a Q_0 of 3.78 b, (3) the ¹⁰⁰Y g_K predicted for constant deformation agrees remarkably well with the experimental value, and (4) the g_K values calculated with the Nilsson model agree very well with the experimental g_K values for all three nuclei. These conclusions together give strong support of the simple picture presented here, that the deformation of the deformed core of ⁹⁸Sr is unaffected by the presence of a valence proton, a valence neutron, or one of each. Therefore the saturation of deformation that was recently de-

duced⁵ for even-even $A \approx 100$ Sr nuclei is shown here to be valid for the odd- A and odd-odd $A \approx 100$ nuclei as well. Stated simply, the extra nucleons do not appear to further polarize the shape.

The latter feature can be simply understood from the proton and neutron Nilsson diagrams for $A \approx 100$. For deformations ϵ_2 in the range 0.2–0.4, the energies of the $\pi_{5/2}^{\pm}[422]$ and $\nu_{3/2}^{\pm}[411]$ orbitals are nearly constant—that is, they are “flat” against ϵ_2 . This is clearly seen in the top part of Fig. 2 for $\nu_{3/2}^{\pm}[411]$. There is no binding energy to be gained by increasing the deformation, thus the deformation tends to saturate in the $A \approx 100$ region nearly as soon as these nuclei become deformed at $N \approx 60$. This behavior contrasts markedly with the $A \approx 150$ (rare earth) region where, for example, deformation sets in at $N \approx 90$ but the largest deformation (i.e., the largest Q_0 or the lowest 2^+ energy) does not occur until $N \sim 100$.

There is a very simple origin to this difference between the $A \approx 100$ and $A \approx 150$ regions, lying in the competition between deformation driving forces and the shell degeneracy. In both regions, 8–10 valence neutrons are needed before deformation occurs, since in each region a proton subshell ($Z=38, 40$ for $A \approx 100$ and $Z=64$ for $A \approx 150$) must first be overcome by the p - n interaction. For $A \approx 100$ nuclei the point where this occurs is already near midshell, but such is not the case for $A \approx 150$ nuclei. This can be understood by considering the variation of the low- Ω orbital energy with ϵ_2 . Low- Ω orbitals with high $\langle j \rangle$, as occur at the beginning of each major shell, are equatorial and thus decrease in energy as ϵ_2 increases due to the short range of the nuclear force. Adding neutrons to such “downsloping” orbitals tends to drive the nucleus toward larger deformation. In the $A \approx 100$ region, there are six downsloping neutron orbitals, and at least five are already occupied when deformation sets in at $N \approx 60$. In the $A \approx 150$ region, however, with neutrons in the next higher oscillator shell, there are ten downsloping orbitals and only four are occupied at the onset of deformation at $N \approx 90$, thus adding more neutrons leads to still larger deformations. Figure 2 illustrates this point by showing the contrasting behavior of the neutron orbitals that lie closest to the Fermi surface at the onset of deformation in these two regions.

A saturation of collectivity for $A \sim 100$ nuclei appears to occur for the Sr and Y nuclei at $N=60, 61$. As we have shown above, the three “valence” nuclei ^{99}Sr , ^{99}Y , and ^{100}Y all have values of Q_0 that are consistent with the Q_0 of 3.78(6) b deduced⁵ for the deformed band in ^{98}Sr . As discussed in Ref. 5, recent data^{17,18} on ^{100}Sr show that saturation for Sr also extends to $N=62$. [Rms radii derived from laser spectroscopic studies¹⁷ indicate that ^{98}Sr and ^{100}Sr have nearly identical rms deformations $\langle \beta^2 \rangle^{1/2}$ in the range 0.37–0.38, and a report¹⁸ on a measurement of the lifetime of the ^{100}Sr 2^+ level gave a preliminary $T_{1/2}$ of 3.9(5) ns, corresponding to $Q_0=3.81(24)$ b.] The three heaviest known Sr isotopes (with $N=60, 61, 62$) appear to have identical values of Q_0 , thus identical deformations. (The actual value of this deformation depends upon the type of deformation assumed.¹⁵) A pure quadrupole¹⁵ deformation β_2 (as in Ref. 5) gives a β_2 of 0.38 for a Q_0 of 3.8 b. It is clearly of interest to measure $E2$

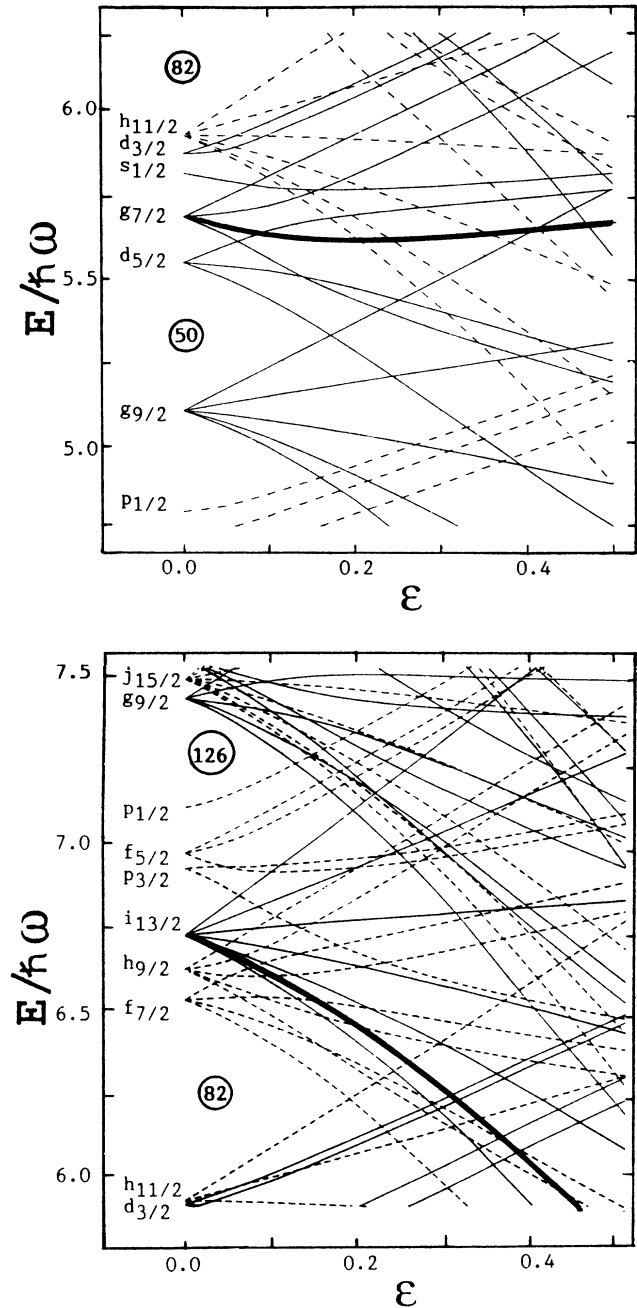


FIG. 2. *Top*: Neutron Nilsson diagram ($\kappa=0.066, \mu=0.35$) for neutron-rich $A \approx 100$ nuclei. The thick line is $\nu_{3/2}^{\pm}[411]$, the $N=61$ orbital for $\epsilon \approx 0.3$. *Bottom*: Neutron Nilsson diagram (Ref. 19) for the $A \approx 150$ rare-earth nuclei. The thick line is $\nu_{3/2}^{\pm}[651]$, the $N=91$ orbital for $\epsilon \approx 0.2$.

strengths for Sr nuclei with $N > 62$ to determine if the collectivity decreases as expected.

In summary, the present determination of $M1$ strengths is possible only due to a fast-timing technique^{2–4} that permits measurements of lifetimes much shorter than 100 ps. The intrinsic g factors deduced for ^{99}Y , ^{99}Sr , and ^{100}Y indicate a constant core deformation

and thus extend the saturation of deformation from even-even Sr nuclei⁵ towards odd-*A* and odd-odd nuclei of Sr and Y. The contrast between the immediate saturation in the $A \approx 100$ region and the gradual increase of deformation in the rare-earth region is explained by simple arguments based on the slope of the valence Nilsson or-

bitals at the onset of deformation in the two regions.

This work was supported by the U. S. Department of Energy under Contract Nos. DE-AC02-76CH00016 and W-7405-ENG-82.

*Present address: The Studsvik Science Research Laboratory, S-61182 Nyköping, Sweden.

¹*Nuclear Structure of the Zirconium Region*, edited by J. Eberth, R. A. Meyer, and K. Sistemich (Springer-Verlag, Berlin, 1988).

²H. Mach, R. L. Gill, and M. Moszyński, *Nucl. Instrum. Methods* **A280**, 49 (1989).

³M. Moszyński and H. Mach, *Nucl. Instrum. Methods* **A277**, 407 (1989).

⁴H. Mach, M. Moszyński, and R. L. Gill (unpublished).

⁵H. Mach *et al.*, *Phys. Lett. B* **230**, 21 (1989).

⁶H. Mach *et al.*, *Phys. Rev. Lett.* **63**, 143 (1989); M. Büscher *et al.*, *Phys. Rev. C* **41**, 1115 (1990).

⁷G. Lhersonneau *et al.*, *Z. Phys. A* **332**, 243 (1989).

⁸F. K. Wahn, J. C. Hill, and R. F. Petry, *Phys. Rev. C* **31**, 621 (1985).

⁹R. A. Meyer *et al.*, *Nucl. Phys.* **A439**, 510 (1985).

¹⁰G. D. Goulden, Ph.D. thesis, University of Oklahoma, 1987 (unpublished).

¹¹F. K. Wahn *et al.*, *Phys. Rev. C* **36**, 1118 (1987).

¹²R. F. Petry *et al.*, *Phys. Rev. C* **37**, 2704 (1988).

¹³Sadek Zeghib *et al.*, *Phys. Rev. C* **36**, 939 (1987).

¹⁴K. L. Kratz, V. Harms, A. Wahn, and P. Möller, *Phys. Rev. C* **38**, 278 (1988).

¹⁵K. E. G. Löbner, M. Vetter, and V. Hönig, *Nucl. Data Tables* **A7**, 495 (1970).

¹⁶I. Ragnarsson, *Proceedings of the International Conference on Nuclei Far From Stability*, Leysin, Switzerland, 1970, CERN Report No. 70-30, 1970, p. 847.

¹⁷R. E. Silverans *et al.*, *Phys. Rev. Lett.* **60**, 2607 (1988).

¹⁸G. Lhersonneau *et al.*, *Verh. Dtsch. Phys. Ges.* **24(VI)**, 26 (1989).

¹⁹*Table of Isotopes*, 7th ed., edited by C. Lederer and V. S. Shirley (Wiley, New York, 1978), Appendix VI, p. 39.